International Journal of Thermophysics, Vol. 7, No. 4, 1986

Application of Critical-Region Scaling to Pure-Component Equations of State[1]

D. D. Erickson[2] and T. W. Leland[2]

A critical scaling method for equations of state developed by Fox at the National Bureau of Standards has been extended to predict thermodynamic properties and all of the first and second derivatives of the chemical potential and density. This is done by using a new damping function and developing expressions which avoid all numerical evaluations of the derivatives needed in calculating thermodynamic properties. Using this procedure, an analytical 32-constant equation of state was scaled in the critical region for pure light hydrocarbons and for carbon dioxide. The BWRS equation was scaled for heavier hydrocarbons. Calculations of the saturated vapor and liquid densities of methane in the region from 175 K to the critical temperature of 190.5 K were improved, and the mean absolute error decreased from 0.153 without scaling to 0.031 with scaling. Other derivative properties were also improved in the critical region for several of the lighter pure hydrocarbons.

KEY WORDS: carbon dioxide; critical region; equation of state; hydrocarbons; scaling.

1. INTRODUCTION

During the past two decades several technological developments have appeared which require equations of state capable of predicting accurate *P–V–T* and thermodynamic properties near the critical conditions for both pure components and mixtures. In current engineering practice, mixture properties are obtained from classical pure-component equations of state by two principal methods. The first of these replaces the constants in a pure-component equation of state with composition-dependent parameters

---

[1] Paper presented at the Ninth Symposium on Thermophysical Properties, June 24–27, 1985, Boulder, Colorado, U.S.A.

[2] Department of Chemical Engineering, Rice University, Houston, Texas 77251, U.S.A.

0195-928X/86/0700-0911$05.00/0

and the resulting equation is used to calculate mixture properties. The second method uses the reduced form of a pure-component equation of state as a reference fluid and assumes that dimensionless properties of the reference fluid are identical to those of the mixture when properly defined pseudocritical functions are used to form the reduced parameters of the reference. Although these mixture procedures give good results at conditions outside the critical region, there are some unsolved theoretical problems in modifying them to apply at conditions close to a critical locus. Consequently, this paper deals only with pure components as a necessary first step in the development of a procedure for accurate property predictions for mixtures at conditions near a critical line.

2. METHOD

The shape of the coexistence curve predicted by an analytical equation of state for a pure component can be significantly improved in the critical region by the method of Fox [1]. This method consists of transforming an analytical equation of state into a nonanalytical equation in a manner which preserves the classical behavior at conditions far from the critical but obeys scaling laws near the critical. This transformation is based on a state function, ψ, which measures the displacement or "distance" from the pure component critical point. The ψ function is defined as

$$\psi = P - P_c - \rho_c(\tilde{\mu} - \tilde{\mu}_c) - \tilde{s}_c(T - T_c) \tag{1}$$

The subscript c in Eq. (1) denotes a value at the critical point. The $\tilde{\mu}$ term in Eq. (1) is a residual chemical potential, defined as

$$\tilde{\mu} = (\mu - \mu^*) + RT\ln(\rho v_0) \tag{2}$$

In Eq. (2) μ is the chemical potential, v_0 is a unit volume, and the asterisk indicates a property which the fluid at a specified temperature and density would have if it obeyed the ideal-gas law at these conditions. The $\tilde{s}$ term is a residual entropy defined as

$$\tilde{s} = \rho\{(s - s^*) + R[1 - \ln(v_0\rho)]\} \tag{3}$$

where s is the molar entropy. The distance function, ψ, is zero both at the critical point and near the spinodal curve within the two-phase region. Outside the spinodal curve, ψ is positive and becomes infinitely large far from the critical point. The nonclassical equation of state can now be defined in terms of the following set of parametric equations:

$$T' = T_c + (T - T_c)\, g^{\theta} \tag{4}$$

$$\tilde{\mu}' = \tilde{\mu}(\rho_c, T') + [\tilde{\mu} - \tilde{\mu}(\rho_c, T)]\, g^{\phi} \tag{5}$$

$$P' = P + \rho_c(\tilde{\mu}' - \tilde{\mu}) + \tilde{s}_c(T' - T_c) \tag{6}$$

In Eqs. (4), (5), and (6) nonclassical properties are denoted by primes. The θ and ϕ terms in Eqs. (4) and (5) are functions of the critical exponents defined as

$$\theta = \frac{2\alpha}{2-\alpha} \tag{7}$$

$$\phi = 1 - 2\beta\left[1 + \left(\frac{\alpha}{2-\alpha}\right)\right] \tag{8}$$

The critical exponent α describes the isochoric heat capacity divergence at the critical, and the critical exponent β describes the approach of the saturated liquid and saturated vapor densities to the critical density, as shown below in Eqs. (9) and (10):

$$c_v \sim (T - T_c)^{-\alpha} \qquad \text{at } \rho = \rho_c \qquad \text{when } T > T_c \tag{9}$$

$$(\rho_L - \rho_c) \sim (T_c - T)^{\beta} \sim (\rho_v - \rho_c) \qquad \text{when } T < T_c \tag{10}$$

where

$$\beta = 0.353 \qquad \text{and} \qquad \alpha = 1/7. \tag{11}$$

The symbol g, defined as the damping function, is a function of ψ only. The function g is zero at the critical point and monotonically increases to a value of unity as displacement from the critical increases. Consequently, at conditions far from the critical: $T' \to T$ and $P' \to P$, and the parametric Equations (4)–(6) then give properties described by the classical equation of state.

Fox's original form of the damping function was defined as follows:

$$g = \left[\frac{(\psi/P_c)^{\lambda/4}}{w + (\psi/P_c)^{\lambda|4}}\right]^{1/\lambda} = \left[1 + w\left(\frac{P_c}{\psi}\right)^{\lambda/4}\right]^{-1/\lambda} \tag{12}$$

where w and λ are adjustable constants which are fitted to experimental data. This damping function becomes proportional to the fourth root of ψ, as the critical point is approached. Therefore, nonclassical properties become scaled replacements for classical properties near the critical by means of the transforms in Eqs. (4)–(6). This damping function was tested by using the Jacobsen and Stewart 32-constant BWR equation [2] with methane constants determined by Ely and Hanley [3]. This equation, when scaled using Eq. (12), predicts the shape and location of the coexistence curve accurately, but it fails to predict accurate derivative properties, especially in what is called the "crossover" region between the critical point and conditions where the original unscaled equation is satisfactory. In this crossover region, Eq. (12) predicts derivatives of P–V–T properties poorly. The predicted residual constant-volume heat capacity, for example, has some spurious discontinuities in its slope in this region.

In this paper an improved damping function g was developed which gives more accurate P–V–T properties including their derivatives in the crossover region and connects smoothly with these properties and derivatives in the classical region. This revised damping function is

$$\begin{aligned} g &= \exp\left\{\left(\frac{v}{v+(\psi/P_c)^n}\right)\ln\left[1+w\left(\frac{P_c}{\psi}\right)^{\lambda/4}\right]^{-1/\lambda}\right\} \\ &= \left[1+w\left(\frac{P_c}{\psi}\right)^{\lambda/4}\right]^{-v/\lambda[v+(\frac{\psi}{P_c})^n]} \end{aligned} \tag{13}$$

where v, n, w, and λ are adjustable constants. This improved damping function in Eq. (13) approaches the critical point in the same manner as Fox's original damping function, but in the crossover region it approaches the classical region like an exponential function.

The four constants in Eq. (13) have been fitted to experimental data on the isobaric and isochoric heat capacities, speed of sound, pressure, density, isochoric slopes of P vs T, isothermal slopes of P vs ρ, and saturation boundaries for the six compounds: methane, ethane, propane, isobutane, n-butane, and carbon dioxide. The 32-constant BWR equation of state is used as the unscaled equation for all of these substances except n-pentane and n-hexane. For n-pentane and n-hexane the analytic Benedict–Webb–Rubin–Starling [4] (BWRS) equation of state was used. The fitted parameters which accompany these equations are shown in Table I. In Fox's original paper, various nonanalytic properties were obtained by numerical evaluation of the first and second derivatives of the three properties in Eqs. (4)–(6). In this work, exact expressions for five different nonanalytic properties have been found. An expression for the density can be found by differentiation of Eq. (6) with respect to Eq. (5), as follows:

$$\rho' = \left(\frac{\partial P'}{\partial \tilde{\mu}'}\right)_{T'} = \rho_c + \frac{(\rho-\rho_c)}{X} g^{-\phi} \tag{14a}$$

where

$$\begin{aligned} X = 1 &+ f\phi(\rho-\rho_c)[\tilde{\mu}(\rho, T) - \tilde{\mu}(\rho_c, T)] \\ &+ \frac{(T-T_c)\,\theta f}{\rho_c}\left\{\rho_c(\tilde{s}-\tilde{s}_c) + (\rho-\rho_c)\left[\left(\frac{\partial P}{\partial T}\right)_{\rho_c} - \tilde{s}(p_c, T)\right]\right\} \end{aligned} \tag{14b}$$

Table I. Fitted Constants for the Revised Damping Function, Eq. (13)[a]

Component	T_c (K)	ρ_c (g-mol · L^{-1})	w	λ	ν	n
Methane	190.555	10.15	0.012237	3.8275	0.47631	0.04091
Ethane	305.33	6.800	0.02640	2.5803	1.4138	0.09665
Propane	369.85	4.995	0.0085929	4.53473	0.8756	0.00044062
Isobutane	407.85	3.860	0.00233	3.798	0.5697	4.1434
n-Butane	425.16	3.920	0.008933	2.5881	0.8825	0.16835
Pentane	469.65	3.30	0.126055	6.6073	0.21925	0.06797
Hexane	507.68	2.50	0.050327	5.7068	0.5699	1.1348
Carbon dioxide	304.21	10.60	0.08772	3.0422	0.06495	0.01637

[a] Experimental data used in developing this table were selected from over 100 sources. A list of these can be obtained from the authors.

and

$$f=\left(\frac{\partial g}{\partial \psi}\right)\frac{1}{g} \tag{14c}$$

An expression for the nonanalytic entropy is obtained by differentiating Eq. (5) with respect to Eq. (4), as shown below:

$$\begin{aligned}\tilde{s}' = -\rho'\left(\frac{\partial \tilde{\mu}'}{\partial T'}\right)_{P'} &= \tilde{s}_c+\frac{(\rho'-\rho_c)}{\rho_c}\Bigg\{\tilde{s}(\rho_c, T')-\left(\frac{\partial P(T')}{\partial T'}\right)_{\rho_c} \\ &\quad + g^{\phi-\theta}\left[\frac{\rho_c(\tilde{s}-\tilde{s}_c)}{\rho-\rho_c}-\tilde{s}(\rho_c, T)+\left(\frac{\partial P}{\partial T}\right)_{\rho_c}\right]\Bigg\}\end{aligned} \tag{15}$$

The second-order derivative properties are obtained in a similar manner, by differentiating Eqs. (14) and (15) with respect to Eqs. (4)–(6) as follows:

$$\begin{aligned}\left(\frac{\partial P'}{\partial \rho'}\right)_{T'} = \left(\frac{\rho'}{\rho}\right)\left(\frac{\rho-\rho_c}{\rho'-\rho_c}\right)^3 g^{-\phi}\Bigg(&\left(\frac{\partial \rho}{\partial P}\right)_T\left[1+\frac{(\rho_c\tilde{s}-\rho\tilde{s}_c)(T-T_c)\,\theta f}{\rho}\right]^2 \\ &- 2\left(\frac{\partial \rho}{\partial T}\right)_P\frac{(\rho-\rho_c)(T-T_c)\,\theta f}{\rho}\left[1+\frac{(\rho_c\tilde{s}-\rho\tilde{s}_c)(T-T_c)\,\theta f}{\rho}\right] \\ &+ \frac{(\rho-\rho_c)^2}{\rho}\,\{(E-f\theta)+(X)(f(\theta-2\phi)-E) \\ &+ \phi f[\tilde{\mu}(\rho, T)-\tilde{\mu}(\rho_c, T)] \\ &\times(\rho-\rho_c)\,f(\phi-\theta)+\theta^2 f^2(T-T_c)^2\,c_p''\}\Bigg)^{-1}\end{aligned} \tag{16a}$$

where

$$E = \left(\frac{\partial f}{\partial \psi}\right)\frac{1}{f} \tag{16b}$$

$$c_{\mathrm{p}}'' = \frac{\rho(c_{\mathrm{p}} - c_{\mathrm{p}}^{*}) + R\rho}{T} + (\rho - \rho_{\mathrm{c}})\left[\frac{1}{\rho_{\mathrm{c}}}\left(\frac{\partial^2 P}{\partial T^2}\right)_{\rho_{\mathrm{c}}} - \frac{c_{\mathrm{v}}(\rho_{\mathrm{c}}, T) - c_{\mathrm{v}}^{*}}{T}\right] \tag{16c}$$

Similarly

$$\begin{aligned}
\left(\frac{\partial \rho'}{\partial T'}\right)_{P'} = {} & \left(\frac{\rho_{\mathrm{c}}\tilde{s}' - \rho'\tilde{s}_{\mathrm{c}}}{\rho' - \rho_{\mathrm{c}}}\right)\left(\frac{\partial \rho'}{\partial P'}\right)_{T'} + \left(\frac{\rho' - \rho_{\mathrm{c}}}{\rho - \rho_{\mathrm{c}}}\right)^2 \\
& \times g^{\phi - \theta}\Biggl(\left(\frac{\partial \rho}{\partial P}\right)_T \left(\frac{\rho\tilde{s}_{\mathrm{c}} - \rho_{\mathrm{c}}\tilde{s}}{\rho - \rho_{\mathrm{c}}}\right)\left[1 + \left(\frac{T - T_{\mathrm{c}}}{\rho}\right)(\rho_{\mathrm{c}}\tilde{s} - \rho\tilde{s}_{\mathrm{c}})\,\theta f\right] \\
& + \left(\frac{\partial \rho}{\partial T}\right)_P \left[1 + \frac{2(T - T_{\mathrm{c}})\,\theta f}{\rho}(\rho_{\mathrm{c}}\tilde{s} - \rho\tilde{s}_{\mathrm{c}})\right] \\
& - (T - T_{\mathrm{c}})\,\theta f(\rho - \rho_{\mathrm{c}})\,c_{\mathrm{p}}'' + \left(\frac{(\rho - \rho_{\mathrm{c}})\,f(\phi - \theta)}{\rho_{\mathrm{c}}}\right) \\
& \times \Biggl\{\rho_{\mathrm{c}}(\tilde{s} - \tilde{s}_{\mathrm{c}} + (\rho - \rho_{\mathrm{c}})\left[\left(\frac{\partial P}{\partial T}\right)_{\rho_{\mathrm{c}}} - \tilde{s}(\rho_{\mathrm{c}}, T)\right]\Biggr\}\Biggr)
\end{aligned} \tag{17}$$

and also,

$$\begin{aligned}
\left(\frac{\partial \tilde{s}'}{\partial T'}\right)_{P'} = {} & \left(\frac{\tilde{s}' - \tilde{s}_{\mathrm{c}}'}{\rho' - \rho_{\mathrm{c}}}\right)\left(\frac{\partial \rho'}{\partial T'}\right)_{P'} + \frac{(\rho' - \rho_{\mathrm{c}})}{\rho_{\mathrm{c}}}\Biggl\{\frac{[c_{\mathrm{v}}(\rho_{\mathrm{c}}, T') - c_{\mathrm{v}}^{*}(T')]}{T'}\,\rho_{\mathrm{c}} \\
& - \left[\frac{\partial P^2(T')}{\partial (T')^2}\right]_{\rho_{\mathrm{c}}}\Biggr\} + \left(\frac{\rho' - \rho_{\mathrm{c}}}{\rho - \rho_{\mathrm{c}}}\right) g^{\phi - 2\theta} \\
& \times \Biggl(c_{\mathrm{p}}''\left[1 - \frac{g^{\theta}(T - T_{\mathrm{c}})\,\theta f}{\rho'}(\rho_{\mathrm{c}}\tilde{s}' - \rho'\tilde{s}_{\mathrm{c}})\right] + \frac{(\rho_{\mathrm{c}}\tilde{s} - \rho\tilde{s}_{\mathrm{c}})}{\rho(\rho - \rho_{\mathrm{c}})^2}\left(\frac{\partial \rho}{\partial P}\right)_T \\
& \times \left\{(\rho_{\mathrm{c}}\tilde{s} - \rho\tilde{s}_{\mathrm{c}}) - \frac{(\rho_{\mathrm{c}}\tilde{s}' - \rho'\tilde{s}_{\mathrm{c}})\,\rho g^{\theta}}{\rho'}\left[1 + \frac{(T - T_{\mathrm{c}})\,\theta f(\rho_{\mathrm{c}}\tilde{s} - \rho\tilde{s}_{\mathrm{c}})}{\rho}\right]\right\} \\
& - \frac{1}{\rho(\rho - \rho_{\mathrm{c}})}\left(\frac{\partial \rho}{\partial T}\right)_P \Biggl\{2(\rho_{\mathrm{c}}\tilde{s} - \rho\tilde{s}_{\mathrm{c}})\left[1 - \frac{(T - T_{\mathrm{c}})\,\theta f g^{\theta}(\rho_{\mathrm{c}}\tilde{s}' - \rho'\tilde{s}_{\mathrm{c}}}{\rho'}\right] \\
& - \frac{(\rho_{\mathrm{c}}\tilde{s}' - \rho'\tilde{s}_{\mathrm{c}})\,\rho g^{\theta}}{\rho'}\Biggr\} + f(\phi - \theta)\frac{(\rho_{\mathrm{c}}\tilde{s}' - \rho'\tilde{s}_{\mathrm{c}})\,g^{\theta}}{\rho_{\mathrm{c}}\rho'} \\
& \times \Biggl\{\rho_{\mathrm{c}}(\tilde{s} - \tilde{s}_{\mathrm{c}}) + (\rho - \rho_{\mathrm{c}})\left[\left(\frac{\partial P}{\partial T}\right)_{\rho_{\mathrm{c}}} - \tilde{s}(\rho_{\mathrm{c}}, T)\right]\Biggr\}\Biggr)
\end{aligned} \tag{18}$$

Using Eqs. (14a)–(14c) along with Eqs. (4)–(6), a procedure can be developed for relating the nonanalytic properties of a scaled equation of state to the analytic properties of a conventional classical equation. For example, suppose values are selected for the nonanalytic conditions T' and P'. The accompanying analytic properties T and P of the original classical equation can be assumed, as a first trial, to be equal to the selected nonanalytic values T' and P'. From these trial T and P values, the distance function ψ is calculated from Eq. (1) and is then used to evaluate the improved damping function g in Eq. (13). A new set of T and P values are then obtained by simultaneous solution of Eqs. (4) and (6), with μ' in Eq. (6) evaluated from Eq. (5). This simultaneous solution can be done either by successive substitution or by Newton–Raphson techniques. These new T and P values are used to repeat this procedure until convergence.

The same type of calculation can be made to find the analytic values of T and ρ in a classical equation which accompany the preassigned values of T' and ρ' for a scaled nonanalytic equation. In this case, Eq. (14) for ρ' is used in place of Eq. (6). The first trial values of T and ρ are set equal to T' and ρ'. These trial values are then used to calculate all terms needed in a simultaneous solution of Eqs. (4) and (14) to obtain new values of T and ρ. These values then are used to repeat the process, which is continued to convergence.

After a consistent set of T, ρ, T', and ρ' values are obtained in this manner, all other nonanalytic properties such as P', s', derivatives of P'–V'–T' properties, and all residual thermodynamic properties can be obtained by using Eq. (6) and Eqs. (15)–(18) for the nonanalytic form of the classical equation of state.

Some of the results obtained with this method are presented in this paper. Figure 1 shows the coexistence curve for methane. The inner curve is obtained from the unscaled 32-constant BWR equation and the outer curve is predicted by its scaled form. The experimental data points are enclosed by the boxes. Unscaled equations of state predict a coexistence curve which is always too pinched near the critical point. The scaling always improves this shape by flattening the coexistence dome at the critical point.

The data points in Fig. 2 show the isochoric slopes for methane obtained from the experimental data of Gammon and Douslin [5]. As Fig. 2 shows, scaling makes a significant improvement in predicting this derivative property. The classical equation falls between the two branches of the scaled curve and the data points. It cannot properly model the singularity in the isochoric slope at the critical point, and the scaled results are in much better agreement with the data.

Figure 3 shows the isothermal slope of pressure vs density for

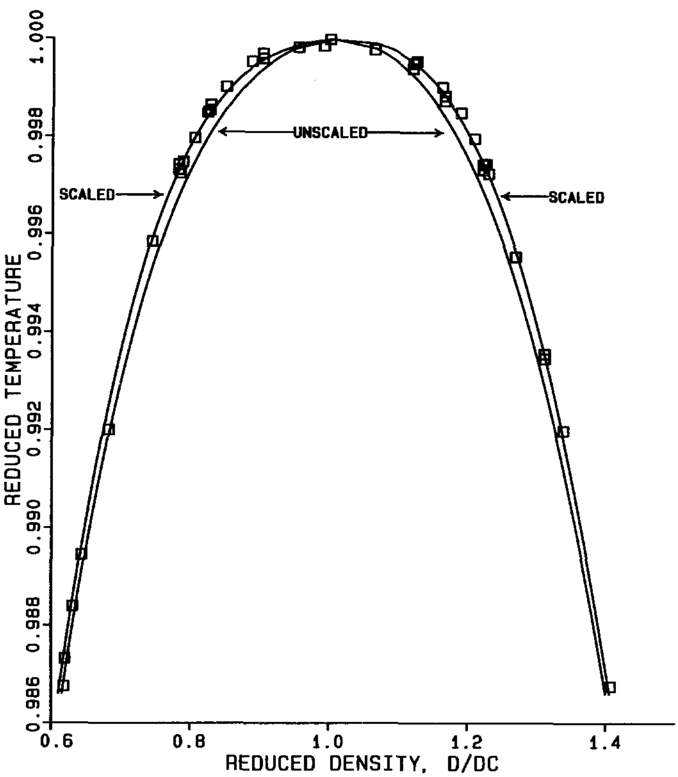

Fig. 1. Methane phase boundary.

methane. As before, the scaled equation, the lower of the two curves, gives much better results. Because of the difference between analytic and nonanalytic critical exponents, the nonanalytic isothermal slope approaches zero at the critical point much faster than the classical result.

Figure 4 depicts the isochoric heat capacity slightly above the critical temperature. This figure shows that scaling gives more nearly the right shape to the curve on each side of the critical density. In this particular case, the slope appears too large at the critical point. There are two plausible reasons for this. The first is the experimental difficulty in measuring simultaneously the heat capacity, which is becoming infinitely large near the critical point, and the density, which is subject to large fluctuations. A second source of error is inherent in the unscaled equation of state. The 32-constant BWR equation for methane predicts a critical density around 10.23 g-mol $\cdot$ L^{-1}, while the true critical density is closer to 10.15 g-mol $\cdot$ L^{-1}. This explains why the scaled curves seem to be shifted to the right in all of the Figures presented here. The distance function ψ is

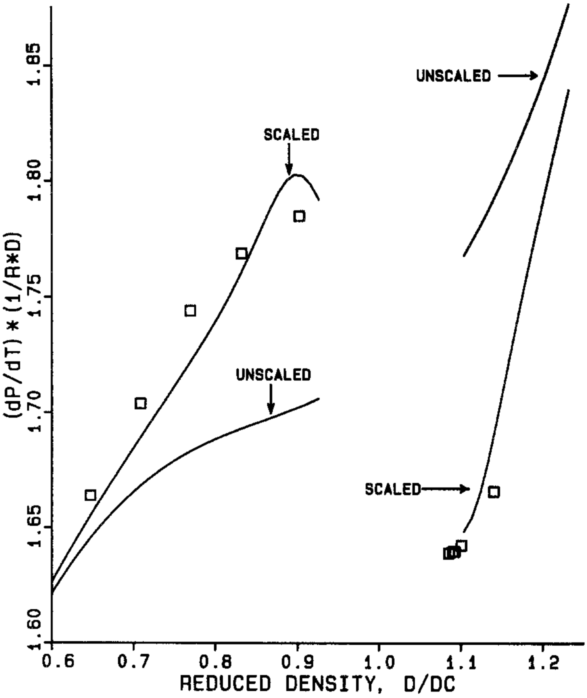

Fig. 2. Methane isochoric slope $(\partial P/\partial T)_\rho$ at the reduced temperature of 0.999711. The experimental data points, which are enclosed by the small squares, were measured by Gammon and Douslin [5].

affected strongly by the location of the critical density as predicted by the unscaled equation. For this scaling procedure to be most successful, an accurate critical point prediction by the unscaled equation of state is essential.

A more fundamental problem in predicting heat capacities near the critical is the fact that scaling itself is inadequate to account for all aspects of the heat capacity behavior in this region. This is explained by Chapela and Rowlinson [6] and Nicoll [7]. Analyses of the problem by Wegner [8] and by Ley-Koo and Green [9] have shown that two types of correction to the classical heat capacity are needed. For the constant-volume heat capacity, c_v, these two corrections are (i) the scaling correction in terms of $[(T-T_c)/T_c]^{-\alpha}$, where α is the critical exponent $\simeq 0.14$; and (ii) a series of "correction-to-scaling" terms in which the leading term is proportional to $[(T-T_c)/T_c]^{\Delta}$ with the exponent $\Delta = 0.5$, as developed by Wegner.

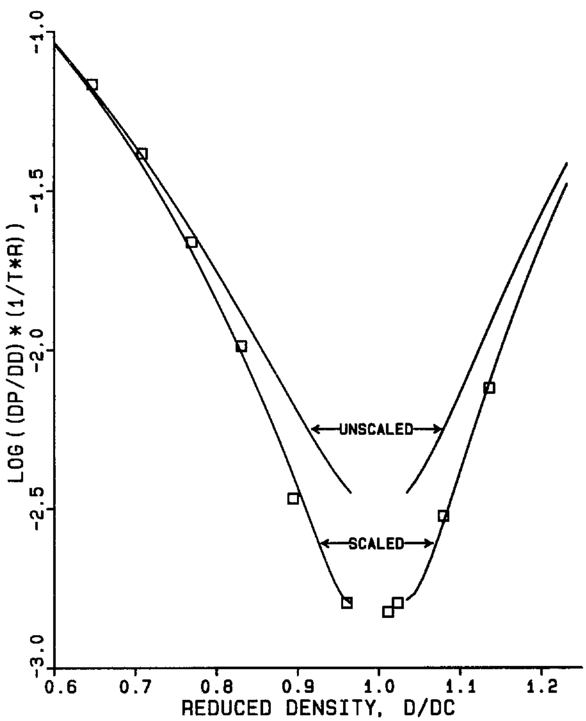

Fig. 3. Methane isothermal slope $(\partial P/\partial \rho)_T$ at the reduced temperature of 1.001548. The experimental data points, which are enclosed by the small squares, were measured by Gammon and Douslin [5].

Because the higher-order terms in this series are difficult to evaluate, Wegner has shown that the correction-to-scaling series can be approximated by the leading term in $[(T-T_c)/T_c]^{\Delta}$ plus a constant.

Moldover [10] has tested this idea and pointed out that in a critical-region c_v expression which consists only of a scaling term with the exponent α, a single correction-to-scaling term with the exponent Δ, and a constant term, the coefficients in the expression cannot be determined unambiguously from experimental data. Furthermore, the constant term does not correspond to a general background contribution which exists outside the critical region. This observation is supported by the work of Lipa et al. [11], who fit c_v data for CO_2 in the critical region to an expression involving only a scaling correction with the exponent α and a constant term. The leading temperature-dependent correction to scaling with the exponent Δ was omitted entirely. Although the constant term is

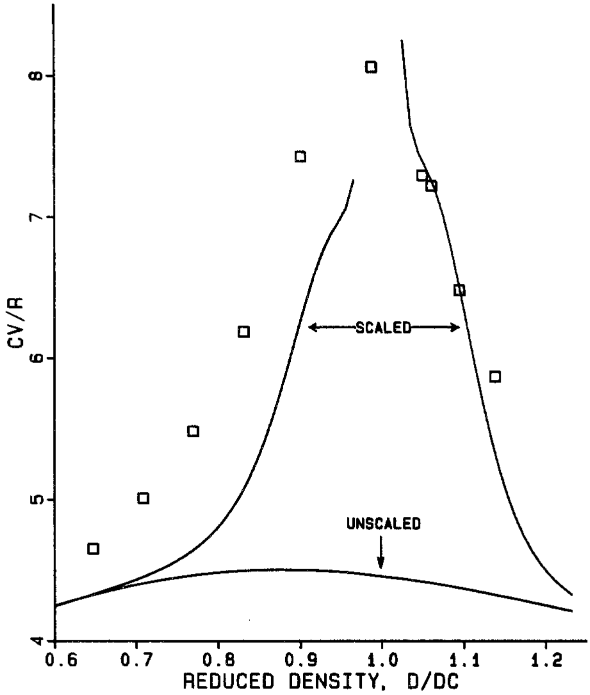

Fig. 4. Methane isochoric heat capacity (C_V) at the reduced temperature of 1.000394. The experimental data points, which are enclosed by the small squares, were measured by Gammon and Douslin [5].

double valued at the critical with one value to be used when $T < T_c$ and another to be used when $T < T_c$, the fit to the experimental data is as good as that obtained when the leading correction to scaling term is included.

Consequently, the parametric equations used in this work involve only a single scaling correction. Considering the accuracy of the data available for fitting parameters in these equations and the inability of classical equations of state to predict accurate critical volumes, a more elaborate procedure is not justified at this time.

3. CONCLUSIONS

Some general comments can be made about this method, based on the pure components studied. In all cases, this procedure makes significant improvements in predictions of the density, isochoric slopes of P vs T, and isothermal slopes of P vs ρ. Predictions for isochoric heat capacity were also improved in comparison with those of the unscaled version, but in most cases there are still large errors near the critical. Predictions for pressure and isobaric heat capacity either were slightly improved or showed no improvement. Therefore it appears that this scaling procedure is most useful in improving properties that were nonsingular in derivations from classical equations of state. An important feature of the improved damping function developed here is that even for the derivative properties, the transition through the crossover region from nonanalytic to classical behavior is very smooth. This represents an important improvement over earlier theories.

ACKNOWLEDGMENT

The authors appreciate the support of this research at Rice University by the Gas Research Institute.

REFERENCES

1. J. R. Fox, *Fluid Phase Equil.* **14**:45 (1983).
2. R. T. Jacobsen and R. J. Stewart, *J. Phys. Chem. Ref. Data* **2**:757 (1973).
3. J. Ely and H. J. M. Hanley, *Ind. Engr. Chem. Fund.* **4**:323 (1981).
4. K. E. Starling, *Fluid Properties for Light Petroleum Systems* (Gulf, Houston, Tex., 1973).
5. B. Gammon and J. Douslin, *Chem. Phys.* **64**:203 (1976).
6. G. A. Chapela and J. S. Rowlinson, *Trans. Faraday Soc.* **70**:584 (1974).
7. J. F. Nicoll, *Phys. Rev.* **A24(4)**:2203 (1981).
8. F. J. Wegner, *Phys. Rev.* **B5**:4529 (1972).
9. M. Lay-Koo and M. S. Green, *Phys. Rev.* **A16**:2483 (1977).
10. M. R. Moldover, *Phase Transitions: Cargese 1980*, M. Levy, J. C. LeGuillou, and J. Zinn. Justin, eds. (Plenum Press, New York, 1982), p. 63.
11. J. A. Lipa, C. Edwards, and M. J. Buckingham, *Phys. Rev.* **A15**:778 (1977).